

See discussions, stats, and author profiles for this publication at: <https://www.researchgate.net/publication/8198390>

Dihydrogen and Methane Elimination from Adducts Formed by the Interaction of Carbenium and Silylium Cations with Nucleophiles

ARTICLE *in* JOURNAL OF THE AMERICAN CHEMICAL SOCIETY · NOVEMBER 2004

Impact Factor: 12.11 · DOI: 10.1021/ja040127e · Source: PubMed

CITATIONS

14

READS

9

2 AUTHORS, INCLUDING:



Igor S. Ignatyev

Saint Petersburg State University

69 PUBLICATIONS 729 CITATIONS

SEE PROFILE

Dihydrogen and Methane Elimination from Adducts Formed by the Interaction of Carbenium and Silylium Cations with Nucleophiles

Igor S. Ignatyev[§] and Henry F. Schaefer III*

Contribution from the Center for Computational Chemistry, University of Georgia,
Athens, Georgia 30602

Received May 6, 2004; E-mail: hfs@uga.edu

Abstract: Stationary points for reactions $R'R''HX^+ + YH \rightarrow [R'R''X-Y]^+ + H_2$ (I) and $R'(CH_3)HX^+ + YH \rightarrow [R'HX-Y]^+ + CH_4$ (II) ($R', R'' = CH_3, H$; $X = C, Si$; $Y = CH_3O, (CH_3)_2N$, and C_6H_5) are located and optimized by the B3LYP/aug-cc-pVDZ method. A similar mechanism was found to be operative for both types of reactions with $X = C$ and $X = Si$. Formation of the intermediate (adduct) results in the transfer of electron density from the electron-rich bases to the X atoms and in the growth of a positive charge on a hydrogen atom attached to Y. This mobile proton may shift from Y to X, and the relative energies of transition states for elimination reactions (ΔE_0^{TS}) depend on the ability of the X atom to retain this proton. Therefore, ΔE_0^{TS} grows on going from Si to C and with increasing numbers of methyl substituents. For $X = C$, the ΔE_0^{TS} value for both reactions correlates well with the population of the valence orbitals of X in a wide range from -44 kcal/mol (methyl cation/benzene) to 31 kcal/mol (isopropyl cation/methanol). For $X = Si$ this range is more narrow (from -19 to -5.0 kcal/mol), but all ΔE_0^{TS} values are negative with the exclusion of silylium ion/benzene systems, adducts of which are π - rather than σ -complexes. The energy minima for product complexes for H_2 elimination are very shallow, and several are dissociative. However, complexes with methane which exhibit bonding between X and the methane hydrogen are substantially stronger, especially for systems with $X = Si$. The latter association energy may reach 8 kcal/mol ($Si \cdots H$ distance is 2 \AA).

Introduction

Formation of the adducts of carbenium and silylium cations with bases (condensation) is the most favorable first step of an important class of ion–molecule reactions.^{1–11} Among these systems, the most studied are reactions of carbenium cations with arenes, due to the role of the resulting arenium ions as intermediates in subsequent electrophilic substitution reactions.^{12,13} Arenium ions are also characterized as stable species in superacidic media.^{12–14} Both experimental¹⁷ and theoretical^{18–21} studies of these ions reveal that their structures may be described

as a σ -complex with the protonated or alkylated carbon of the benzene ring having nearly sp^3 character.

Less is known about the adducts produced by the interaction of silylium cations (R_3Si^+) with arenes, although their structures have been vividly discussed in connection with the problem of the existence of free silylium cations in condensed phases. The crystal structures of stable triethylsilylium cations showed no coordination of these species to the complex anions, and this allowed Lambert and co-workers to claim that the free silylium cation had been characterized.^{22–24} This conclusion was disputed by Schleyer and Apeloig,¹⁹ Cremer,²⁵ Pauling,²⁶ and Olah.²⁷ In the course of this discussion, the structure of the complex between the silylium ion and benzene became the subject of theoretical studies.^{19–21,26–29} It was found that the main structural

[§] Permanent address: Department of Chemistry, Radiochemistry Laboratory, St. Petersburg State University, St. Petersburg 199034, Russia.

- (1) Speranza, M. *Chem. Rev.* **1993**, *93*, 2933.
- (2) Cacace, F. *Acc. Chem. Res.* **1988**, *21*, 215.
- (3) Cacace, F.; Crestoni, M. E.; de Petris, G.; Fornarini, S.; Grandinetti, F. *Can. J. Chem.* **1988**, *66*, 3099.
- (4) Attina, M.; Cacace, F.; Ricci, A. *J. Am. Chem. Soc.* **1991**, *113*, 5937.
- (5) Cacace, F.; Crestoni, M. E.; Fornarini, S. *J. Am. Chem. Soc.* **1992**, *114*, 6776.
- (6) Sen Sharma, D. K.; Ikuta, S.; Kebarle, P. *Can. J. Chem.* **1982**, *60*, 2325.
- (7) Stone, J. M.; Stone, J. A. *Int. J. Mass Spectrom. Ion Processes* **1991**, *109*, 247.
- (8) Blair, I. A.; Bowie, J. H.; Trenerry, V. C. *J. Chem. Soc., Chem. Commun.* **1979**, 230.
- (9) Blair, I. A.; Trenerry, V. C.; Bowie, J. H. *Org. Mass Spectrom.* **1980**, *15*, 15.
- (10) Stone, J. A. *Mass Spectrom. Rev.* **1997**, *16*, 25.
- (11) Cheng, Q.-F.; Stone, J. A. *Int. J. Mass Spectrom. Ion Processes* **1997**, *165*, 195.
- (12) Taylor, R. *Electrophilic Aromatic Substitution*; Wiley: West Sussex, U.K., 1990.
- (13) Brouwer, D. M.; Mackor, E. L.; McLean, C. In *Carbocation Ions*; Olah, G. A., Schleyer, P. v. R., Eds.; Wiley: New York, 1970; Vol. 2, p 837.
- (14) Olah, G. A.; Kuhn, S.; Pavlath, A. *Nature* **1956**, *178*, 693.

- (15) Olah, G. A.; Schlosberg, R. H.; Porter, R. D.; Mo, Y. K.; Kelley, D. P.; Matescu, G. D. *J. Am. Chem. Soc.* **1972**, *94*, 2034.
- (16) Olah, G. A. *Angew. Chem., Int. Ed. Engl.* **1995**, *34*, 1393.
- (17) Baenziger, N. C.; Nelson, A. D. *J. Am. Chem. Soc.* **1968**, *90*, 6602.
- (18) Hehre, W. J.; Pople, J. A. *J. Am. Chem. Soc.* **1972**, *94*, 6901.
- (19) Schleyer, P. v. R.; Buzek, P.; Müller, T.; Apeloig, Y.; Siehl, H.-U. *Angew. Chem., Int. Ed. Engl.* **1993**, *32*, 1471.
- (20) Miklis, P. C.; Ditchfield, R.; Spencer, T. A. *J. Am. Chem. Soc.* **1998**, *120*, 10482.
- (21) Lambert, J. B.; Zhang, S.; Stern, C. I.; Huffman, J. C. *Science* **1993**, *260*, 1917.
- (22) Lambert, J. B.; Zhang, S. *Organometallics* **1994**, *13*, 2430.
- (23) Reed, C. A.; Xie, Z.; Bau, R.; Benesi, A. *Science* **1993**, *262*, 402.
- (24) Reed, C. A.; Kim, K.-C.; Stoyanov, E. S.; Stasko, D.; Tham, F. S.; Mueller, L. J.; Boyd, P. D. W. *J. Am. Chem. Soc.* **2003**, *125*, 1796.
- (25) Olsson, L.; Cremer, D. *Chem. Phys. Lett.* **1993**, *215*, 433.
- (26) Pauling, L. *Science* **1994**, *263*, 983.
- (27) Olah, G. A.; Rasul, G.; Li, X.-Y.; Buchholz, H. A.; Sanford, G.; Prakash, G. K. S. *Science* **1994**, *263*, 983.

difference between carbenium and silylium complexes with arenes is the substantially greater weight of the π -complex resonant form in the silylated arenes. The relative contribution of σ - and π -complexes may be described by the angle between the C–Si(C) bond and the benzene ring plane. This angle of elevation of the substituent for carbenium ions is ca. 55°, while that for silylium ions is larger than 75°. ^{19–21}

Vibrationally excited metastable ions formed by the reactions between cations and bases may undergo unimolecular decomposition. Numerous mass-spectrometric studies of metastable $[\text{CH}_3\text{YH}]^+$ ions ($\text{Y} = \text{OH}, \text{NH}_2, \text{SH}$), formed either by the condensation reaction of methyl cations or by the protonation of methanol and methylamine, have been carried out. These studies show that the most abundant positively charged species are formed by the loss of YH (the inverse of the condensation reaction) and by the loss of molecular hydrogen. ^{30–35} Although all the reactions $\text{CH}_3^+ + \text{YH} \rightarrow \text{CH}_2\text{Y}^+ + \text{H}_2$ ($\text{Y} = \text{OH}, \text{NH}_2, \text{SH}$) are exothermic, only the reactions with NH_3 and H_2S were observed to proceed with rates comparable to the theoretical rate for capture collisions, while the reaction with water was not observed. ³¹ In 1973, Bowers, Chesnavich, and Huntress ³¹ applied a quasiequilibrium theory (QET) for the estimation of the barrier heights for the H_2 elimination from metastable $[\text{CH}_3\text{YH}]^+$ ions ($\text{Y} = \text{OH}, \text{NH}_2, \text{SH}$). They estimated that the barrier for water lies only 4 ± 3 kcal/mol below the reactant level ($\text{CH}_3^+ + \text{H}_2\text{O}$). Since it is possible that the excess energy of condensation may not be completely randomized before dissociation of the adduct, this barrier may be too high for H_2 elimination to occur in the system of a water molecule. Nobes and Radom ³⁶ optimized stationary points on the potential energy surface (PES) of these reactions by the SCF/6-31G(d) method. They found that the barrier height for H_2 elimination from $[\text{CH}_3\text{OH}_2]^+$ is 69 kcal/mol (1.4 kcal/mol above reactants). Estimations of this barrier height based on the optimization of stationary points by the MP2/6-31G(d,p) method gave a slightly lower barrier (67 kcal/mol). ³⁷

Decomposition pathways for protonated isopropylamine, ³⁸ ethanol, ³⁹ and ethylamine ⁴⁰ have also been studied theoretically. The presence of alkyl groups with the number of carbon atoms larger than one in these metastable ions gives way for another channel of their fragmentation in addition to the H_2 elimination, i.e., the loss of alkane (methane for the ions studied).

All the above studies deal with the decomposition of metastable adducts of carbenium ions with water or ammonia. A few studies on similar reactions for silylium ions and/or both types of cations with larger bases may be found. The H_2

elimination from the adduct of SiH_3^+ and benzene was observed by Allen and Lampe. ^{41,42} In the mass spectrometric study of this reaction, they found that the main product of the SiC_6H_9^+ ion decomposition at low reactant kinetic energies is the SiC_6H_7^+ ion, produced by the H_2 elimination from the adduct. Experiments with SiD_3^+ ions have shown that the silabenzyl cation, $\text{C}_6\text{H}_5\text{SiH}_2^+$, is formed by a 1,2 molecular hydrogen elimination. ^{41,42} Ion cyclotron resonance studies of the reaction between the Me_3Si^+ cation, produced by the electron impact on tetramethylsilane and methanol, have been reported. These studies show that one of the most abundant products of the decomposition of the $[\text{Me}_3\text{SiO(H)Me}]^+$ adduct is the $[\text{Me}_2\text{SiOMe}]^+$ ion, formed by the elimination of methane (MeH). ⁴³ Experiments with CD_3OD have shown that methane is formed from one methyl of the trimethylsilyl group and a hydrogen atom of methanol. The elimination of H_2 from the MeH_2Si^+ –methanol adduct was also reported in the work.

Thus, although some experimental evidence for elimination of dihydrogen and alkanes from adducts formed by the interaction of carbenium and silylium ions exists, the findings are not systematic and are obtained under different experimental conditions. On the other hand, theoretical predictions for these processes exist only for the reactions of methyl and ethyl cations with water and ammonia. Both experimental and theoretical results show that the H_2 elimination is possible for the reaction of carbenium cations with ammonia, but not for water. ^{30–35} Neither experimental nor theoretical predictions exist for the reactions with stronger bases, such as methanol and amines. Are these reactions possible for these nucleophiles? For reactions with benzene, H_2 elimination was reported for SiH_3^+ . ^{41,42} Is it possible for CH_3^+ and for alkyl-substituted carbenium and silylium ions? How does the methyl substitution at X ($\text{X} = \text{C}, \text{Si}$) affect the barrier heights for both pathways of unimolecular decomposition? With the aim of answering these and some other questions, we have undertaken the systematic study of stationary points at the PES of the systems in which $\text{H}_n\text{Me}_{(3-n)}\text{C}^+$ as well as $\text{H}_n\text{Me}_{(3-n)}\text{Si}^+$ cations ($n = 1, 2$) interact with representatives of the three widely used types of bases, i.e., methanol, dimethylamine, and benzene.

Theoretical Methods

The DFT method combining Becke's three-parameter exchange functional ⁴⁴ with the LYP correlation functional ⁴⁵ (B3LYP) was used throughout this work. For the assessment of this method, for the most studied systems of methyl cation with water and ammonia, second-order Møller–Plesset perturbation theory (MP2) ⁴⁶ was also used. Both methods were employed as implemented in the GAUSSIAN 94 program. ⁴⁷ The frozen-core option was used with MP2. The basis sets were the standard Dunning correlation-consistent basis sets, ^{48,49} namely cc-pVnZ and aug-cc-pVnZ, with $n = 2, 3$, and 4.

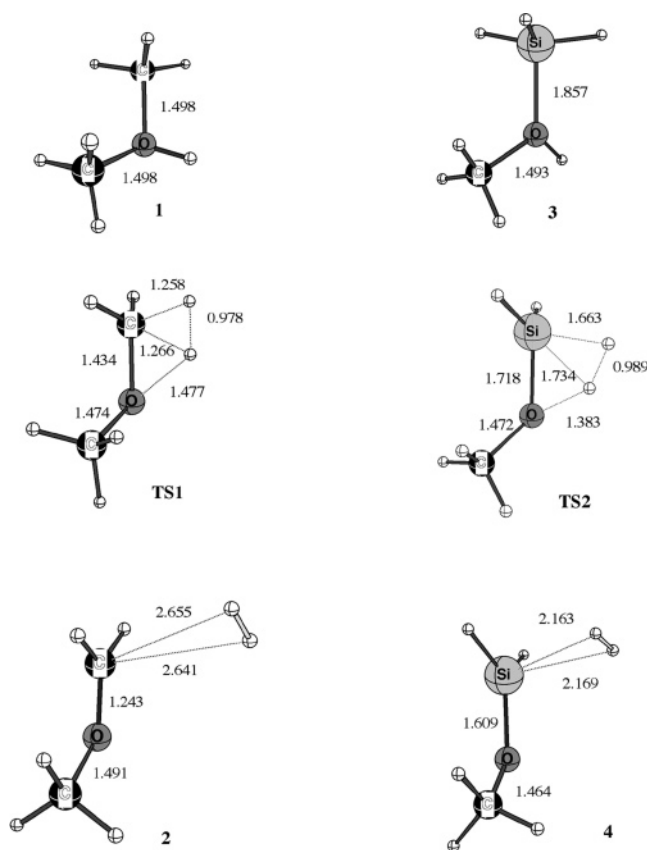
- (28) Olsson, L.; Ottosson, C.-H.; Cremer, D. *J. Am. Chem. Soc.* **1995**, *117*, 7460.
- (29) Smith, W. B. *J. Phys. Org. Chem.* **2002**, *15*, 347.
- (30) Huntress, W. T.; Elleman, D. D. *J. Am. Chem. Soc.* **1970**, *92*, 3565.
- (31) Bowers, M. T.; Chesnavich, W. J.; Huntress, W. T. *Int. J. Mass Spectrom. Ion Phys.* **1973**, *12*, 1.
- (32) Huntress, W. T.; Bowers, M. T. *Int. J. Mass Spectrom. Ion Phys.* **1973**, *12*, 357.
- (33) Huntress, W. T.; Sen Sharma, D. K.; Jennings, K.; Bowers, M. T. *Int. J. Mass Spectrom. Ion Processes* **1977**, *24*, 25.
- (34) Day, R. J.; Krause, D. A.; Jorgensen W. L.; Cooks, R. G. *Int. J. Mass Spectrom. Ion Processes* **1979**, *30*, 83.
- (35) Gilbert, J. R.; van Koppen, P. A. M.; Huntress, W. T.; Bowers, M. T. *Chem. Phys. Lett.* **1981**, *82*, 455.
- (36) Nobes, R. H.; Radom, L. *Chem. Phys.* **1983**, *74*, 163.
- (37) Øiestad, E. L.; Øiestad, A. M. L.; Skaane, H.; Ruud, K.; Helgaker, T.; Uggerud, E.; Vulpis, T. *Eur. Mass Spectrom.* **1995**, *1*, 121.
- (38) Reiner, E. J.; Poirer, R. A.; Peterson, M. R.; Csizmadia, I. G.; Harrison, A. G. *Can. J. Chem.* **1986**, *64*, 1652.
- (39) Swanton, D. J.; Marsden, C. J.; Radom, L. *Org. Mass Spectrom.* **1991**, *26*, 227.
- (40) Øiestad, E. L.; Uggerud, E. *Int. J. Mass Spectrom.* **2000**, *199*, 91.

- (41) Allen, W. N.; Lampe, F. W. *J. Chem. Phys.* **1976**, *65*, 3378.
- (42) Allen, W. N.; Lampe, F. W. *J. Am. Chem. Soc.* **1977**, *99*, 2943.
- (43) Blair, I. A.; Phillipou, G.; Bowie, J. H. *Aust. J. Chem.* **1979**, *32*, 59.
- (44) Becke, A. D. *J. Chem. Phys.* **1993**, *98*, 5648.
- (45) Lee, C.; Yang, W.; Parr, R. G. *Phys. Rev. B* **1988**, *785*.
- (46) Binkley, J. S.; Pople, J. A. *Int. J. Quantum Chem.* **1975**, *9*, 229.
- (47) Frisch, M. J.; Trucks, G. W.; Schlegel, H. B.; Gill, P. M. W.; Johnson, B. G.; Robb, M. A.; Cheeseman, J. R.; Keith, T.; Petersson, G. A.; Montgomery, J. A., Jr.; Raghavachari, K.; Al-Laham, M. A.; Zakrzewski, V. G.; Ortiz, J. V.; Foresman, J. B.; Cioslowski, J.; Stefanov, B. B.; Nanayakkara, A.; Challacombe, M.; Peng, C. Y.; Ayala, P. Y.; Chen, W.; Wong, M. W.; Andres, J. L.; Replogle, E. S.; Gomperts, R.; Martin, R. L.; Fox, D. J.; Binkley, J. S.; Defrees, D. J.; Baker, J.; Stewart, J. P.; Head-Gordon, M.; Gonzalez, C.; Pople, J. A. *Gaussian 94*, Revision C.3; Gaussian, Inc.: Pittsburgh, PA, 1995.

Table 1. Relative Energies of Products (ΔE_0) and Activation Barrier Heights (ΔE_0^{TS}) with Respect to Reactants for the Reaction $\text{CH}_3^+ + \text{YH} \rightarrow \text{CH}_2\text{Y}^+ + \text{H}_2$ ($\text{Y} = \text{OH}, \text{NH}_2$)^a

<i>n</i>	ΔE_0				ΔE_0^{TS}			
	B3LYP		MP2		B3LYP		MP2	
	aug- <i>n</i> Z	<i>n</i> Z	aug- <i>n</i> Z	<i>n</i> Z	aug- <i>n</i> Z	<i>n</i> Z	aug- <i>n</i> Z	<i>n</i> Z
Y = OH								
D	−43.7	−32.7	−41.2	−30.7	−11.1	−2.7	−5.7	−0.2
T	−37.9	−34.5	−36.4	−33.1	−6.3	−2.1	−4.9	−2.8
Q ^b	−36.2	−34.3	−34.7	−33.4	−3.5	−2.1	−4.0	−3.1
expt		−33 ^c	(−29 ^d)			−4 ± 3 ^d		
Y = NH₂								
D	−76.5	−69.2	−75.7	−68.5	−27.7	−22.5	−24.0	−20.4
T	−72.8	−70.4	−72.5	−70.1	−23.2	−21.2	−23.9	−22.6
Q ^b	−71.7	−70.7	−73.0	−70.8	−22.3	−21.4	−23.8	−23.3
expt		−71 ^d				−11 ± 7 ^d		

^a These results are predicted by the B3LYP and MP2 levels with cc-pVnZ (*n*Z) and aug-cc-pVnZ (aug-*n*Z) basis sets (*n* = D, T, Q) and are compared with experimental estimates ($E_0 = E_c + \text{ZPVE}$). All energies are in kcal/mol. ^b E_0 values obtained at the optimized geometry with ZPVE corrections. ^c From the heat of formation of CH_2OH^+ reported in ref 50. ^d Reference 31.

**Figure 1.** Geometrical structures of the stationary points in the $\text{H}_3\text{X}^+ + \text{CH}_3\text{OH}$ system ($\text{X} = \text{C}, \text{Si}$; bond lengths in Å).

Results and Discussion

Since some of the systems considered here are large, a reliable and economical theoretical method should be chosen. The existing experimental estimates of thermochemical parameters for the H_2 elimination reactions from the methyl cation–water (ammonia) adducts allow one to assess the quality of the theoretical approximations. The two most popular methods applied for complex systems, i.e., B3LYP and MP2, give reasonable correlation energies. Both B3LYP and MP2 methods exhibit

Table 2. Relative Energies in kcal/mol (E_e , $E_0 = \Delta E_e + \Delta \text{ZPVE}$) for Stationary Points of the $\text{R}'\text{R}''\text{HX}^+ + \text{CH}_3\text{OH}$ Systems ($\text{R}', \text{R}'' = \text{CH}_3, \text{H}$)

X = C				X = Si		
	no. ^a	ΔE_{e}	ΔE_0		ΔE_{e}	ΔE_0
H_3X^+						
reactants		0	0		0	0
adduct	1	−77.3	−70.0	3	−62.3	−58.6
TS	TS1	−14.4	−13.1	TS2	−13.4	−13.1
complex	2	−50.8	−51.8	4	−35.6	−35.7
products		−48.9	−51.2		−29.2	−32.1
$\text{CH}_3\text{H}_2\text{X}^+$						
reactants		0	0		0	0
adduct	5	−48.3	−42.2	8	−53.2	−49.6
channel for H_2 elimination (I)						
TS	TS3	15.4	16.4	TS5	−9.3	−9.2
complex	6	−28.6	−30.7	9	−31.8	−32.5
products		−27.5	−30.8		−27.7	−30.8
channel for CH_4 elimination (II)						
TS	TS4	9.0	10.3	TS6	−9.4	−9.9
complex	7	−27.9	−25.8	10	−32.9	−30.8
products		−24.6	−23.4		−23.3	−22.8
$(\text{CH}_3)_2\text{HX}^+$						
reactants		0	0		0	0
adduct	11	−32.7	−26.9	14	−46.0	−42.5
channel for H_2 elimination (I)						
TS	TS7	29.7	30.9	TS9	−5.1	−5.0
complex	12	−19.7	−21.8	15	−28.3	−29.4
products		−18.7	−22.2		−25.5	−28.7
channel for CH_4 elimination (II)						
TS	TS8	25.0	26.3	TS10	−4.7	−5.2
complex	13	−25.4	−23.7	16	−30.1	−28.4
products		−23.4	−22.5		−24.1	−23.8

^a Structure numbers as in Figures 1–5.

convergence with increasing *n* within the cc-pVnZ basis sets. However, cc-pVnZ and aug-cc-pVnZ relative energies converge from opposite directions (Table 1). Thus, the extrapolated values for the exothermicity (ΔE_0) of the reactions $\text{CH}_3^+ + \text{YH} \rightarrow \text{CH}_2\text{Y}^+ + \text{H}_2$ ($\text{Y} = \text{OH}, \text{NH}_2$) lie in the 33–34 kcal/mol range for water and 70–71 kcal/mol for ammonia. The latter values coincide well with the reaction exothermicity derived from experimental heats of formation. However, the exothermicity (29 kcal/mol) of the reaction with water reported by Bowers, Chesnavich, and Huntress³¹ and based on the heat of formation of CH_2OH^+ (protonated formaldehyde) differs somewhat from our best estimate. However, the updated value of this heat of formation, reported by Traeger and Holmes,⁵⁰ leads to the reaction exothermicity of 33 kcal/mol, which is in excellent agreement with our results (Table 1).

The experimentally estimated barrier heights for these reactions are uncertain due to several approximations inherent in the quasiequilibrium theory³¹ (Table 1). However, the predicted barrier height with respect to the reactant energy level (ΔE_0^{TS}) for water converges to a value of ca. −3 kcal/mol, which is in good agreement with the experimental estimate. The analogous exothermicity for ammonia reaction, however, is somewhat greater even than the upper value of the experimental estimate. Note that in both cases B3LYP converges to ΔE_0^{TS} values about 1–2 kcal/mol higher than the MP2 results, despite the widespread opinion that B3LYP significantly underestimates barrier heights, primarily for odd-electron systems. In our case,

(48) Dunning, T. H. *J. Chem. Phys.* **1989**, 90, 1007.

(49) Kendall, R. A.; Dunning, T. H.; Harrison, R. J. *J. Chem. Phys.* **1992**, 90, 6796.

(50) Traeger, J. C.; Holmes, J. L. *J. Phys. Chem.* **1993**, 97, 3453.

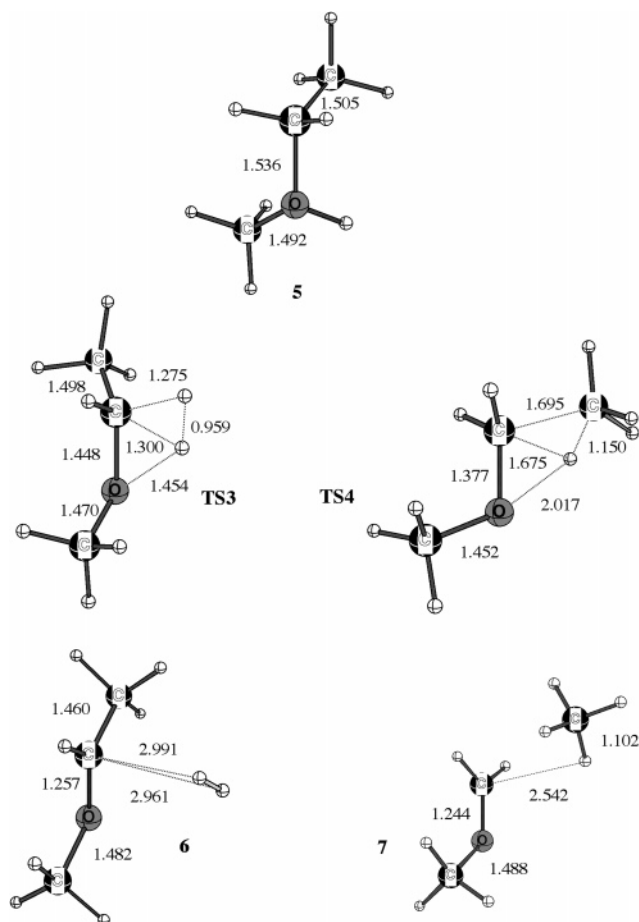


Figure 2. Geometrical structures of the stationary points in the $\text{CH}_3\text{H}_2\text{C}^+ + \text{CH}_3\text{OH}$ system (bond lengths in Å).

some overestimation of barrier heights may be noticed for the cc-pVDZ basis set, but the addition of diffuse functions to this basis set makes the B3LYP barrier heights comparable to those of MP2 (Table 1). One may see that the B3LYP method, even using the cc-pVDZ basis set augmented with diffuse functions, predicts thermochemical parameters with quality comparable that of to much more expensive methods. Below we report the results obtained by the B3LYP/aug-cc-pVDZ method in the study of reactions of carbenium and silylium ions with methanol, dimethylamine, and benzene.

Methanol. Structures of stationary points in the $\text{CH}_3^+ + \text{CH}_3\text{OH}$ and $\text{SiH}_3^+ + \text{CH}_3\text{OH}$ systems are shown in Figure 1. The adducts (**1** and **3**) are formed without barrier, and their association (condensation) is exothermic by 70 and 59 kcal/mol for the $[\text{CH}_3\text{OHCH}_3]^+$ and $[\text{SiH}_3\text{OHCH}_3]^+$ ions, respectively. This energy, stored in the adducts, makes them vibrationally excited (hot) and may lead to their unimolecular decomposition, provided that the barrier heights for these pathways are less than the condensation energy stored in them ($\Delta E_0^{\text{TS}} < 0$). However, as in the case of the $[\text{CH}_3\text{OH}_2]^+$ ion, small negative values of ΔE_0^{TS} may not allow the system to overcome this barrier, due to incomplete randomization of the association energy among the vibrational degrees of freedom. Dodd and Brauman's density of states arguments⁵¹ are also relevant to the inefficiency of the reactions of the complexes.

The formation of a σ bond between cation and nucleophile leads to charge transfer from the base to the X atom of the

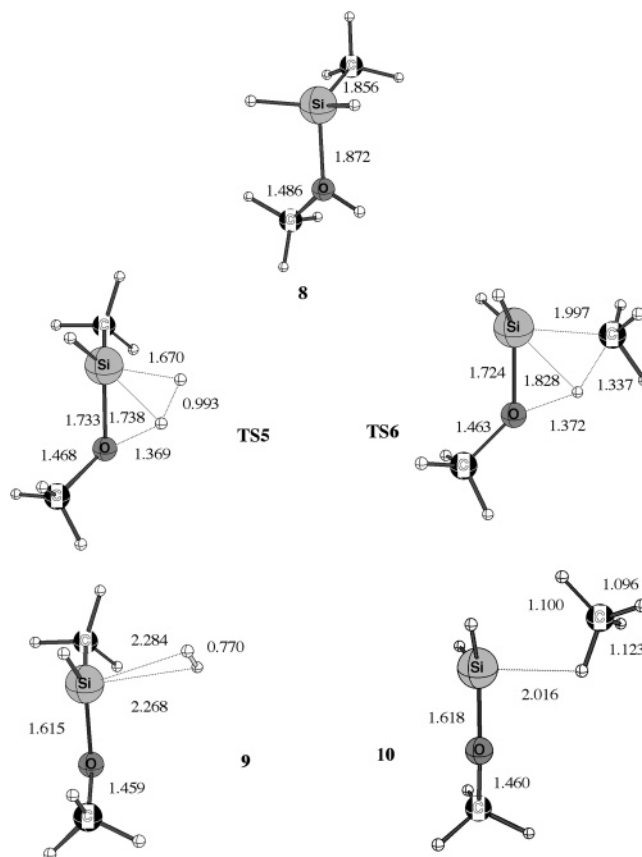


Figure 3. Geometrical structures of the stationary points in the $\text{CH}_3\text{H}_2\text{Si}^+ + \text{CH}_3\text{OH}$ system (bond lengths in Å).

cation. Population analysis based on the natural bond orbital (NBO) method⁵² shows that the natural charge on C increases from 0.29 in the methyl cation to -0.25 in the adduct. The charge transfer for $\text{X} = \text{Si}$ is not so great: from 1.36 in silyl cation to 1.13 in the adduct. This charge transfer is accompanied by a substantial increase of the positive charge on the hydroxyl H; its charge increases from 0.48 in methanol to 0.56 in **1** and to 0.57 in **3**. Note that, despite a considerable difference in the charge transferred from oxygen to X, the growth of positive charge on the hydroxylic hydrogen is even slightly larger for $\text{X} = \text{Si}$.

In the $\text{CH}_3^+ + \text{CH}_3\text{OH}$ system, the only low-energy unimolecular decomposition pathway is the H_2 elimination, since the loss of the methyl cation is the trivial inverse reaction and the other plausible channel, i.e., the loss of proton, is endothermic by 189 kcal/mol. The transition-state geometry for H_2 elimination is similar to those earlier described for the interaction of methyl and ethyl cations with water.^{36,37,39} It is characterized by a shift of the hydroxyl group proton, which became substantially more "mobile" (large positive charge) in the adduct, from oxygen to carbon (**TS1**, Figure 1). The downhill path from this transition state leads to the weak product complex **2** (Figure 1). It is ca. 1 kcal/mol below the product energy level in terms of E_e , but ZPVE corrections reduce this value to 0.6 kcal/mol (E_0 , Table 2). With the basis set superposition error (BSSE) correction⁵³ of 0.4 kcal/mol, there are serious doubts as to the

(51) Dodd, J. A.; Brauman, J. I. *J. Phys. Chem.* **1986**, *90*, 3559.

(52) Reed, A. E.; Weinstock, R. B.; Weinhold, F. *J. Chem. Phys.* **1985**, *83*, 735.

(53) Boys, S. F.; Bernardi, F. *Mol. Phys.* **1970**, *18*, 553.

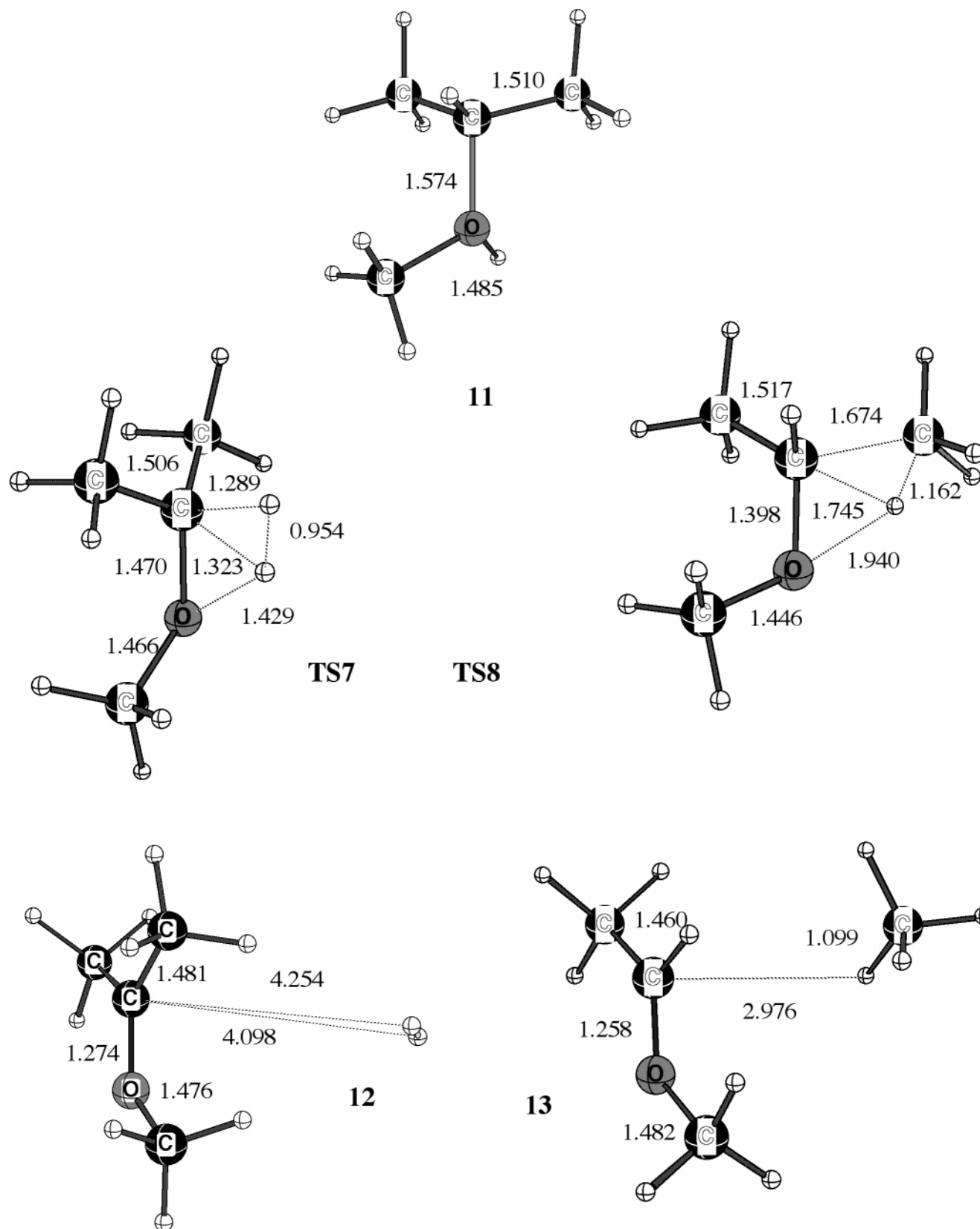


Figure 4. Geometrical structures of the stationary points in the $(\text{CH}_3)_2\text{HC}^+ + \text{CH}_3\text{OH}$ system (bond lengths in Å).

existence of this minimum, even at 0 K. The $[\text{H}_2\text{COCH}_3]^+$ ion (methylated formaldehyde) produced by H_2 loss from the adduct has a short equilibrium CO bond distance (1.242 Å) with a trivalent carbon. The same level of optimization of formaldehyde

gives 1.207 Å. This comparison indicates the predominance of a $\text{H}_2\text{C}=\text{O}(\text{CH}_3)^+$ structure for this cation.

For the $[\text{SiH}_3\text{OHCH}_3]^+$ adduct, one more decomposition channel becomes plausible, i.e., the loss of CH_3^+ . But this

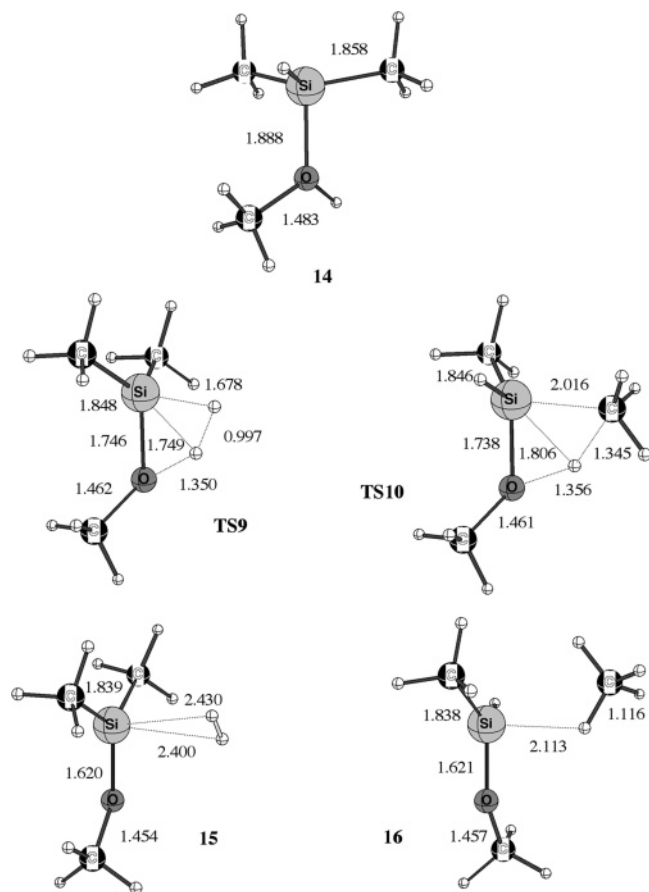


Figure 5. Geometrical structures of the stationary points in the $(\text{CH}_3)_2\text{HSi}^+ + \text{CH}_3\text{OH}$ system (bond lengths in Å).

process is substantially endothermic due to the significantly lower heat of formation of the silyl cation compared to methyl cation and will not be considered here. The transition state for dihydrogen loss from the $[\text{SiH}_3\text{OHCH}_3]^+$ ion (**TS2**, Figure 1) was not described earlier. It differs from that for the methyl cation in the position of the migrating proton. In **TS1**, the $\text{O}\cdots\text{H}$ interatomic distance (1.48 Å) is considerably longer than in **TS2** (1.38 Å). The shorter H–H distance in **TS1** also evidences that this transition state is late compared to **TS2**. This fact reflects higher endothermicity of the $[\text{H}_3\text{XOHCH}_3]^+ \rightarrow [\text{H}_2\text{XOCH}_3]^+ + \text{H}_2$ reaction for $\text{X} = \text{Si}$ (27 vs 19 kcal/mol). The product complex **4** is more tightly bound than that for the carbon counterpart; the hydrogen molecule is retained at shorter distances from the trivalent atom (Figure 1) and is stable toward dissociation by 3.6 kcal/mol, even after applying the ZPVE corrections (BSSE-corrected value is 2.8 kcal/mol). The SiO bond distance in the product ion $[\text{H}_2\text{SiOCH}_3]^+$ (methylated silanone) is 1.602 Å, substantially longer than in $\text{H}_2\text{Si}=\text{O}$ (1.494 Å). This indicates a significantly greater contribution of the $\text{H}_2(\text{CH}_3\text{O})\text{Si}^+$ structure in contrast to methylated formaldehyde.

The replacement of one hydrogen in the methyl and silyl cations by a methyl group results in the stationary point geometries depicted in Figures 2 and 3. This substitution leads to lower binding energies for the adducts of the MeH_2X^+ ($\text{X} = \text{C}, \text{Si}$) cations (**5** and **8**) and longer X–O interatomic separations. Such an effect may be rationalized by assuming the greater electron-withdrawing ability of the methyl group compared to hydrogen, and it is reflected in the decrease of the NBO valence orbital population from 4.24 to 4.05 for $\text{X} = \text{C}$ and from 2.82

Table 3. Relative Energies in kcal/mol (E_e , $E_0 = \Delta E_e + \Delta\text{ZPVE}$) for Stationary Points of the $\text{R}'\text{R}''\text{HX}^+ + (\text{CH}_3)_2\text{NH}$ Systems ($\text{R}', \text{R}'' = \text{CH}_3, \text{H}$)

	X = C			X = Si		
	no. ^a	ΔE_e	ΔE_0	no. ^a	ΔE_e	ΔE_0
H_3X^+						
reactants		0	0		0	0
adduct	17	−126.7	−118.9	19	−85.6	−80.8
TS	TS11	−34.6	−33.5	TS12	−18.9	−18.8
complex	18	−93.3	−94.1	20	−45.8	−47.0
products		−92.5	−94.1		−43.4	−46.2
$\text{CH}_3\text{H}_2\text{X}^+$						
reactants		0	0		0	0
adduct	21	−86.2	−78.7	24	−74.4	−69.6
channel for H_2 elimination (I)						
TS	TS13	0.4	1.1	TS15	−12.8	−12.7
complex	22	−61.5	−63.0	25	−41.4	−39.8
products		−60.5	−63.2		−37.2	−40.1
channel for CH_4 elimination (II)						
TS	TS14	−4.5	−3.4	TS16	−10.9	−11.2
complex	23	−69.5	−67.3	26	−41.4	−39.8
products		−68.0	−66.3		−37.5	−36.8
$(\text{CH}_3)_2\text{HX}^+$						
reactants		0	0		0	0
adduct	27	−66.6	−59.0	30	−65.3	−60.5
channel for H_2 elimination (I)						
TS	TS17	18.0	19.2	TS19	−7.1	−7.0
complex	28	−45.4	−47.2	31	−33.0	−34.8
products		−44.7	−47.4		−31.6	−34.8
channel for CH_4 elimination (II)						
TS	TS18	12.1	13.6	TS20	−5.0	−5.2
complex	29	−58.2	−55.9	32	−36.3	−34.9
products		−56.6	−54.9		−33.7	−33.1

^a Structure numbers as in Figures 6–10.

to 2.56 for $\text{X} = \text{Si}$ upon methyl substitution. However, the decreases of the binding energy between cation and methanol are not comparable for C and Si. As a result, the adduct for $\text{X} = \text{Si}$ becomes more stable than that for C (Table 2). The inversion of the order of the binding energies between nucleophiles and R_3X^+ cations for $\text{X} = \text{C}$ and $\text{X} = \text{Si}$ on going from $\text{R} = \text{H}$ to $\text{R} = \text{Me}$ was discussed by Basch, Hoz, and Hoz.⁵⁴ They ascribed this effect to the stabilizing hyperconjugative interaction between the vacant orbital of X and the occupied methyl group orbitals. They concluded that this interaction is much stronger in carbenium than in silylium cations.

The increase of ΔE_0^{TS} for H_2 elimination (channel I) for both types of cation accompanies the decrease of the binding energy of the adduct (Table 2). However, while this increase for $\text{X} = \text{C}$ comprises 30 kcal/mol (ΔE_0^{TS} for **TS3** becomes 16 kcal/mol), for $\text{X} = \text{Si}$ it grows by only 4 kcal/mol and remains below the reactant level (**TS5**). The reason for this difference may lie in the well-known ability of silicon to coordinate more than four atoms, not ordinarily the case for carbon. The structures of the discussed transition states show that carbon and silicon atoms increase their coordination. This is completely untypical for carbon, and the withdrawal of electron density dramatically lowers the stability of the transition state. The product complex **6** of the $[\text{MeH}(\text{OMe})\text{Si}]^+$ ion with H_2 becomes unstable, even after ZPVE corrections.

Methyl substitution in these cations gives another opportunity for the shift of the mobile proton of the adduct. The proton may migrate to a methyl group which possesses a significant negative charge (channel II). The transition states for this process

(54) Basch, H.; Hoz, T.; Hoz, S. *J. Phys. Chem. A* **1999**, *103*, 6458.

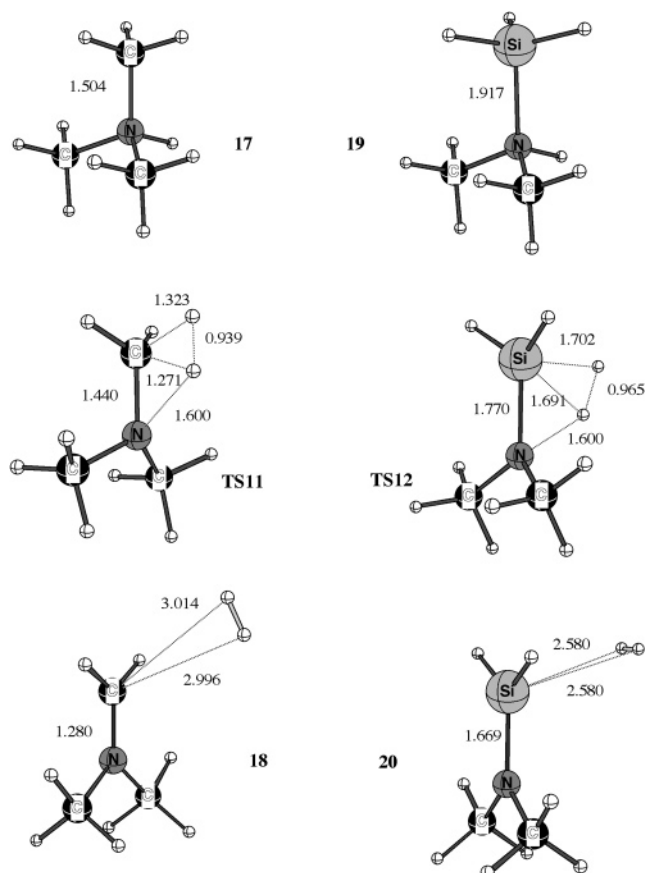


Figure 6. Geometrical structures of the stationary points in the $\text{H}_3\text{X}^+ + (\text{CH}_3)_2\text{NH}$ system ($\text{X} = \text{C}, \text{Si}$; bond lengths in Å).

are depicted in Figure 2 (**TS4**) and Figure 3 (**TS6**). These transition states have pentacoordinated structures similar to those for the H_2 elimination (channel I). However, in the case of methane elimination, the weakly bound ligands are not two hydrogens but rather a methyl group and a hydrogen atom. The barrier heights for channel II are lower than those of channel I by several kilocalories per mole. The similarities in structures and barrier heights of the transition states indicate that the main factors in both processes are the mobility of the hydroxyl proton and the ability of the X atom to retain an additional hydrogen in its coordination sphere.

The product complexes for methane elimination (**7** and **10**) have larger association energies than those for channel I. The methane molecule is bound to the X atom of the $[\text{H}_2(\text{OMe})\text{X}]^+$ ion by one of its hydrogen atoms. This bond is substantially stronger when $\text{X} = \text{Si}$. The complex **10** has a binding energy of 8 kcal/mol (BSSE-corrected value is 7 kcal/mol) and a short (2.02 Å) $\text{Si}\cdots\text{H}$ interatomic distance (Figure 3).

The subsequent substitution for another methyl group gives the stationary points depicted in Figures 4 and 5, and their relative energies are shown in Table 2. The addition of the second methyl group further weakens the bonding between cation and oxygen. The additional withdrawal of electron density from X also manifests itself in the further increase of ΔE_0^{TS} and the decrease of the binding energy of product complexes. Due to a smaller effect of H/Me substitution on electron density around Si, all these tendencies are considerably less pronounced for adducts of silylium ions. In the latter systems, the formation energies decrease by only 4 kcal/mol, while this decrease

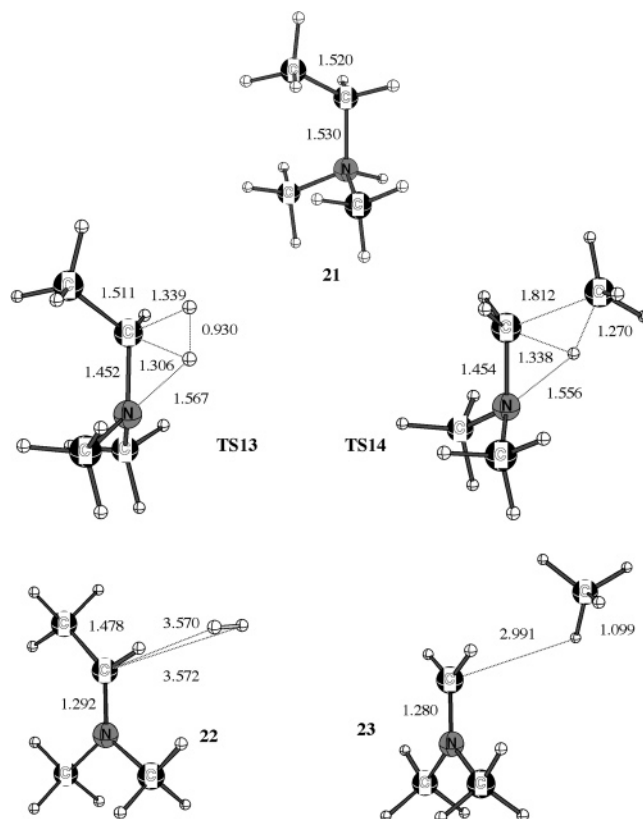


Figure 7. Geometrical structures of the stationary points in the $\text{CH}_3\text{H}_2\text{C}^+ + (\text{CH}_3)_2\text{NH}$ system (bond lengths in Å).

for $\text{X} = \text{C}$ comprises 16 kcal/mol. This comparison makes the $[\text{Me}_2\text{HSiOMe}]^+$ adduct more stable than $[\text{Me}_2\text{HCOMe}]^+$ by 16 kcal/mol. Despite the small increase in ΔE_0^{TS} values for $[\text{Me}_2\text{HSiOMe}]^+$, **TS9** and **TS10** remain negative.

Dimethylamine. Since dimethylamine is a stronger base than methanol (proton affinity of the former is 222 kcal/mol, while that of the latter 180 kcal/mol), its adducts $[\text{R}'\text{R}''\text{HX}-\text{NHMe}_2]^+$ ($\text{R}', \text{R}'' = \text{Me}, \text{H}$) have substantially larger association energies (Table 3). The more effective charge transfer from the n center to the X atom upon the formation of the X–N bond leads to the lowering of ΔE_0^{TS} for H_2 and methane elimination. Note, however, that these barrier heights with respect to the bottom of the adduct potential well are higher than those for methanol. Thus, for the adducts of the H_3C^+ cation, in which this effect is largest, the barrier for the H_2 loss grows from 57 to 85 kcal/mol on going from methanol to dimethylamine. This increase of the barrier height may be rationalized by taking into account the lower positive charge on the hydrogen atom in dimethylamine and its adducts. The NBO population analysis shows that the natural charge of H at oxygen in methanol is 0.48, while that for H of the NH group in dimethylamine is only 0.37. Adduct formation with methyl cation increases this charge to 0.56 for methanol and to 0.45 for dimethylamine. However, the large increase in the association energy of dimethylamine overcomes this increase of the barrier height, and the overall ΔE_0^{TS} value is lowered from –13 kcal/mol in the methyl cation–methanol system to –33 kcal/mol for the corresponding adduct of dimethylamine.

Nevertheless, as is the case for methanol, methyl substitution in cations leads to a sharp decrease in the condensation energy and to the growth of ΔE_0^{TS} . Even for the ethyl cation (**TS13**),

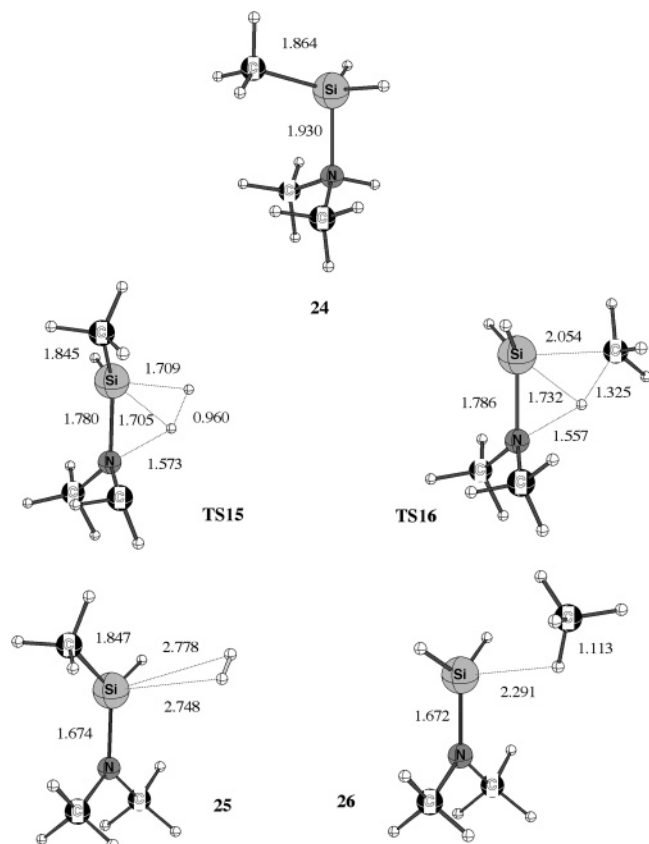


Figure 8. Geometrical structures of the stationary points in the $\text{CH}_3\text{H}_2\text{Si}^+ + (\text{CH}_3)_2\text{NH}$ system (bond lengths in Å).

the value of ΔE_0^{TS} becomes positive. However, similar reactions for silylium cations have negative ΔE_0^{TS} values (Table 3). The structures of the transition states (TS13–TS20) depicted in Figures 7–10 are similar to the corresponding structures for the methanol adducts.

The above observations notwithstanding, significant differences exist in the structures of the product complexes between methanol and dimethylamine (22, 23, 25, 26, 28, 29, 31, 32). These complexes are substantially weaker than the analogous complexes in the case of methanol. This becomes especially clear by comparing the methane complexes for $\text{X} = \text{Si}$, since H_2 exit complexes were also extremely weak for methanol systems. Thus, while the $[\text{H}_2\text{Si}-\text{OMe}]^+ \cdot \text{CH}_4$ complex (10) has an association energy of 8 kcal/mol (Table 2) and a $\text{Si} \cdots \text{H}$ distance of 2.02 Å (Figure 3), in the corresponding $[\text{H}_2\text{Si}-\text{NMe}_2]^+ \cdot \text{CH}_4$ complex (26) the association energy is reduced to 3 kcal/mol (Table 3) and the $\text{Si} \cdots \text{H}$ separation elongates to 2.53 Å (Figure 10). Especially weak are both types of exit complexes in the isopropyl cation–dimethylamine system. The structure type previously found for the exit complexes was not located in this system. The energy minimum was found for the H_2 complex, but it is extremely shallow (Table 3), and the hydrogen molecule therein is instead coordinated to the N atom (28, Figure 9). A new type of coordination is exhibited in the methane complex 29. The hydrogen bond there is formed not by the methane hydrogen and X atom as before, but rather by the H atom at C and the methane carbon. This complex is stable after ZPVE corrections, but its energy ($E_0 = 1.0$ kcal/mol) lies within the limits of the BSSE correction.

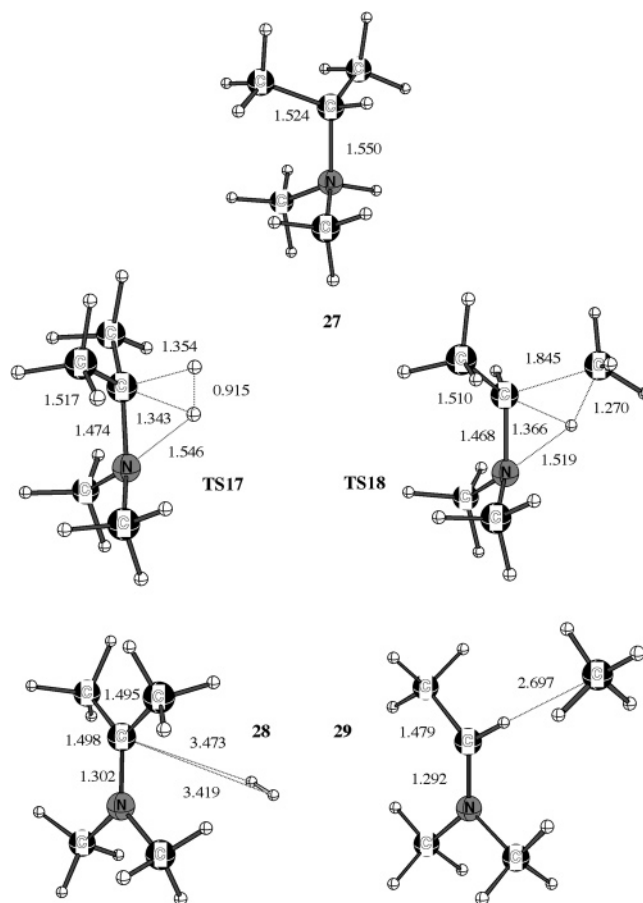


Figure 9. Geometrical structures of the stationary points in the $(\text{CH}_3)_2\text{HC}^+ + (\text{CH}_3)_2\text{NH}$ system (bond lengths in Å).

Benzene. The structural difference between complexes of carbenium and silylium ions with benzene is well known.^{19,20,24,25,27–29} Carbenium cation complexes are typical σ -complexes, while those of silylium ions have predominant π character. This difference is reflected in their structural parameters (Figures 11–15). Carbenium ions have a nearly sp^3 character at the carbon atom forming a bond with cation, while the sp^3 character of the silylated carbon is only partially developed. The angle between the $\text{X}-\text{C}$ bond and the benzene ring plane for methyl cation is 141° (33, Figure 11), while that for silyl cation is 105° (35, Figure 11). In the complex with the ethyl cation (Figure 12), two structures differing in the rotation of the ethyl group around the CC bond were found to have practically the same energy. In the structure of C_s symmetry, the CC bond of the cation is in the trans position to the *ipso*- CH bond of benzene (37). This structure gains stability from weak interactions between hydrogens of the β carbon atom of the ethyl group and carbon atoms of the benzene ring. However, the repulsive interaction between the β carbon atom of the ethyl group bearing a large negative charge (natural charge -0.65) and the π electron density of the benzene ring competes with stabilization by weak $\text{CH} \cdots \text{C}$ interactions. This unfavorable interaction is absent in the structure of C_1 symmetry, in which the CC bond of cation is in the gauche position (37a). Note that these two structures with the same energy have considerably different CC bond lengths (between cation and benzene moieties) and angles between the CC bond and the benzene plane. The structure with the cationic CC in the cis position to

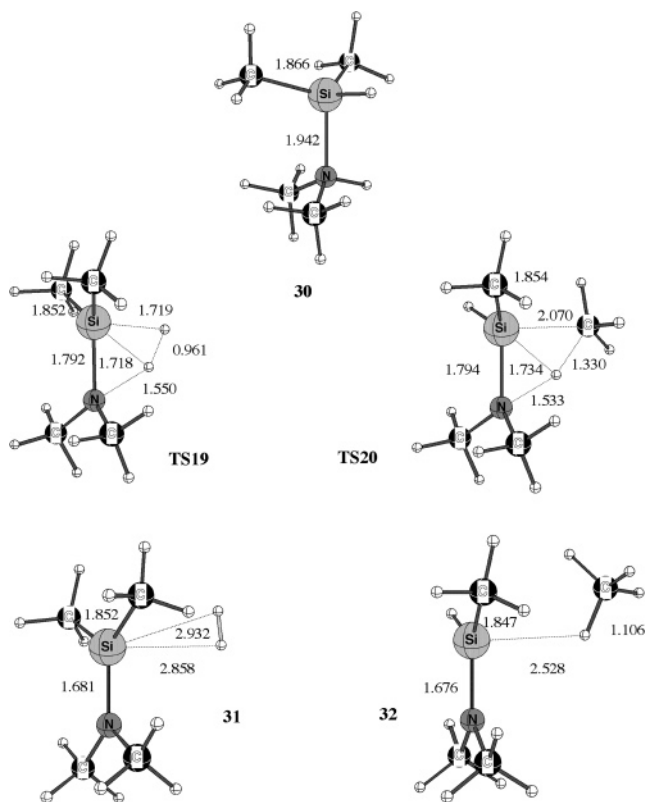


Figure 10. Geometrical structures of the stationary points in the $(\text{CH}_3)_2\text{HSi}^+ + (\text{CH}_3)_2\text{NH}$ system (bond lengths in Å).

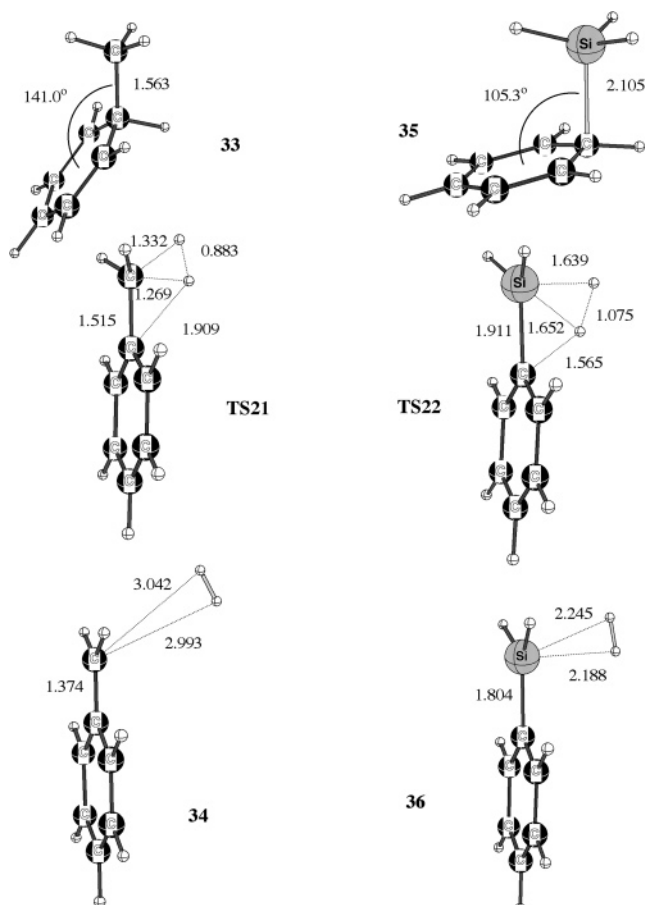


Figure 11. Geometrical structures of the stationary points in the $\text{H}_3\text{X}^+ + \text{C}_6\text{H}_6$ system ($\text{X} = \text{C}, \text{Si}$; bond lengths in Å).

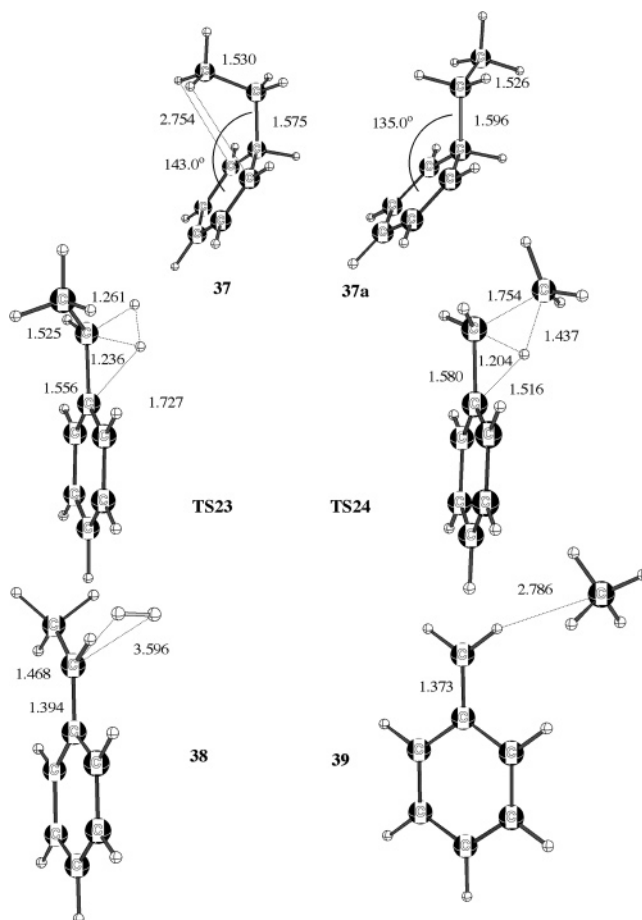


Figure 12. Geometrical structures of the stationary points in the $\text{CH}_3\text{H}_2\text{C}^+ + \text{C}_6\text{H}_6$ system (bond lengths in Å).

the *ipso*-CH bond of benzene is the transition state for the interconversion of **37** and **37a**. In the isopropyl cation–benzene system, the global minimum corresponds to the structure in which one CC bond of the cation is in the trans position (hydrogens weakly interacting with ring carbons), and the other CC bond is in the gauche position (**43**, Figure 14). Earlier a similar structure was found to be a global minimum by Heidrich.⁵⁵

In the complex or adduct of the methylsilyl cation with benzene (Figure 13), the rotamer with a methyl group situated above the benzene plane is less stable by ca. 1 kcal/mol with respect to the structure in which the SiC bond of cation is in the gauche position to the *ipso*-CH bond of the benzene ring (**40**, Figure 13). The preference of the gauche isomer may be understood in terms of the larger atomic separation between cation and benzene and the larger negative NBO charge on the β carbon (−1.16). The isomer with two methyl groups in the gauche positions is also the global energy minimum for the $[\text{Me}_2\text{Si}-\text{C}_6\text{H}_6]^+$ cation (**46**, Figure 15). The association energies of H_3X^+ cations with YH bases follow the order $(\text{CH}_3)_2\text{NH} > \text{C}_6\text{H}_6 > \text{CH}_3\text{OH}$ for $\text{X} = \text{C}$, but $(\text{CH}_3)_2\text{NH} > \text{CH}_3\text{OH} > \text{C}_6\text{H}_6$ for $\text{X} = \text{Si}$ (Table 4). This difference is due to the facts that the complexes for $\text{X} = \text{Si}$ are more π -like than σ -like and the charge transfer from benzene is quite small.

Transition-state structures for the H_2 elimination from the complexes with benzene bear some resemblance to those of methanol and dimethylamine. The transition state in the methyl

(55) Heidrich, D. *Angew. Chem., Int. Ed.* **2002**, *41*, 3208.

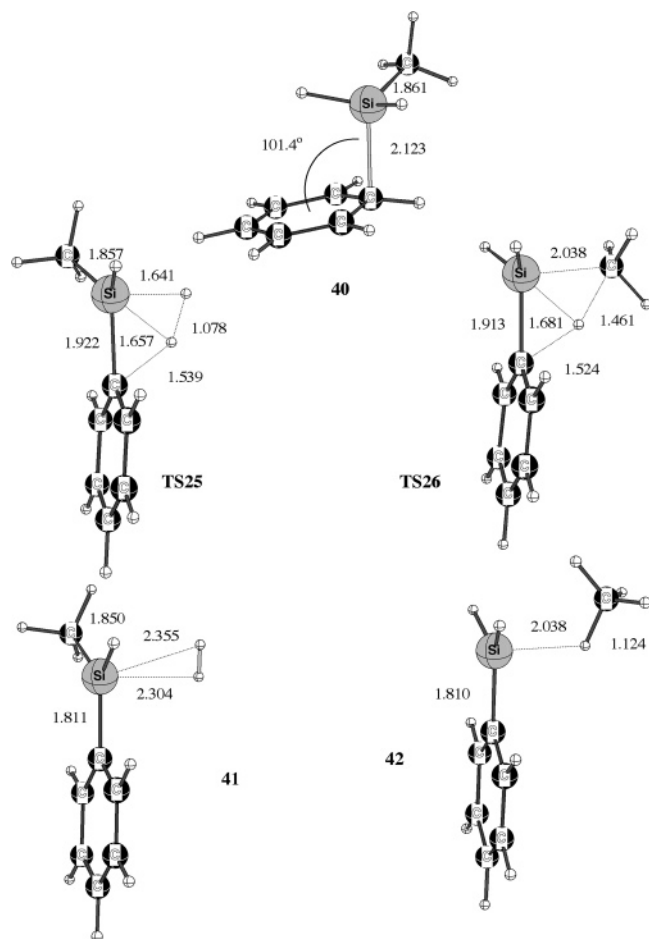


Figure 13. Geometrical structures of the stationary points in the $\text{CH}_3\text{H}_2\text{Si}^+ + \text{C}_6\text{H}_6$ system (bond lengths in Å).

cation–benzene system (the lowest ΔE_0^{TS}) has the largest interatomic distance between the “native” carbon and the migrating proton (TS21, Figure 11). Upon methyl substitution in the cation, the analogous distances become shorter (TS23 in Figure 12, TS27 in Figure 14) but are still substantially longer than those in the corresponding transition states for systems with methanol and dimethylamine. In contrast to the earlier-discussed systems, in which the ΔE_0^{TS} values for methyl-substituted cations were positive for $\text{X} = \text{C}$ but negative for $\text{X} = \text{Si}$, in the silylium ion–benzene systems the ΔE_0^{TS} values become positive, even for the MeH_2Si^+ cation (TS25) (Table 4). In general, the transition state relative energies for silylium ion complexes with benzene lie considerably higher than those of silylium ions with other bases. This is also a manifestation of the specific bonding character in these complexes.

The product complexes are weaker than those for methanol, but stronger than in the dimethylamine system. Among complexes with H_2 , only the complex with silabenzyl cation (36, Figure 11) is stable after ZPVE corrections. However, complexes with CH_4 are more stable, especially those with $\text{X} = \text{Si}$. The complex of silabenzyl cation with methane (42 in Figure 13) has $\Delta E_0 = 4.5$ kcal/mol (3.6 after BSSE correction) and a short $\text{Si}\cdots\text{H}$ distance (2.04 Å). In the methane exit complex of the benzene adducts of the ethyl (39 in Figure 12) and isopropyl (45 in Figure 14) cations, the carbon atom of the cation moiety cannot retain the methane molecule by weak interactions with its hydrogen. Instead, as in the isopropyl cation–dimethylamine

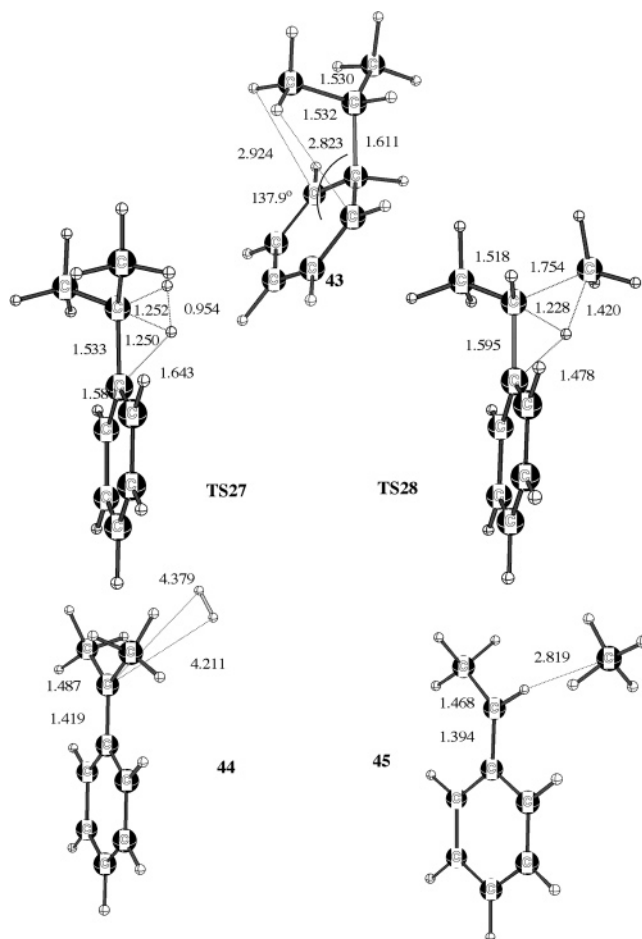


Figure 14. Geometrical structures of the stationary points in the $(\text{CH}_3)_2\text{HC}^+ + \text{C}_6\text{H}_6$ system (bond lengths in Å).

system (29, Figure 9), the energy minimum corresponds to a complex with a weak interaction between the hydrogen atom at the trivalent carbon of the former cation and the methane carbon. Interatomic distances of these $\text{CH}\cdots\text{C}$ interactions are in the 2.7–2.8 Å range, and the dissociation energies of these complexes (ΔE_0) are ca. 1 kcal/mol. However, this value is close to the BSSE correction estimates, and their existence even at 0 K is questionable.

Reaction Mechanisms and Correlation of Barrier Heights to the Electron Density on X Atoms. Summarizing the discussion of the unimolecular decomposition of methanol, dimethylamine, and benzene adducts, we present a correlation between the transition-state levels and certain natural populations of X atoms to which departing hydrogen and methane molecules are coordinated in these transition states (Table 5). All reactions studied in this work have similar mechanisms. During the formation of adducts, a significant amount of electron density is transferred to the X atom of the former cation. The proton of the former base becomes more positively charged and mobile and may migrate to the X atom, forming the transition state in which the X atom becomes pentacoordinated. The relative stability of this transition state depends on the binding ability of X. Upon substitution of H atoms at X for methyl groups, the excess electron density that came from the base is withdrawn by the methyl groups. This weakens the binding ability of X. It appears that this qualitative description is supported by the quantitative correlation of ΔE_0^{TS} with the

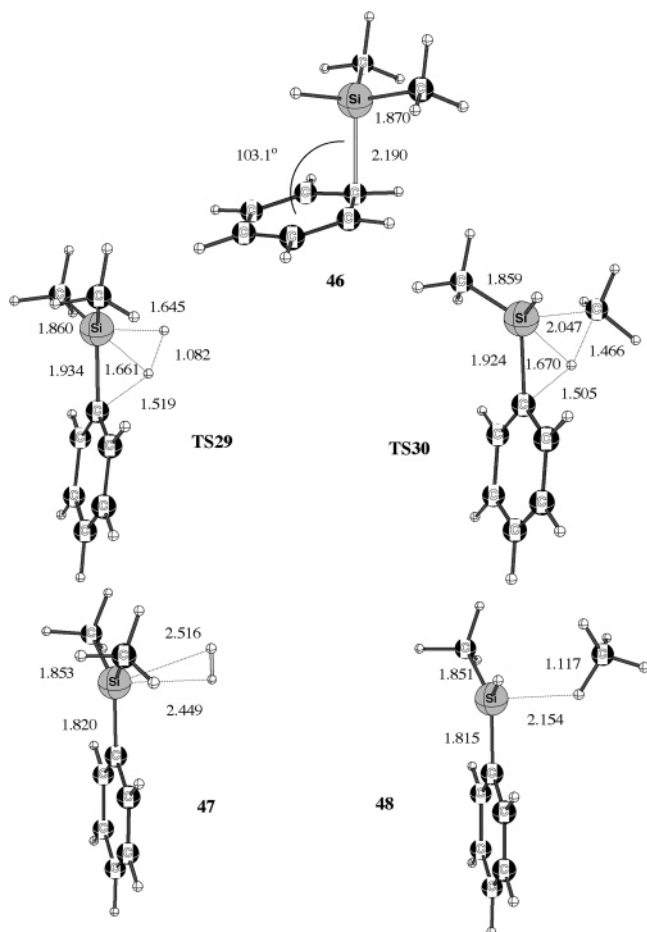


Figure 15. Geometrical structures of the stationary points in the $(\text{CH}_3)_2\text{HSi}^+ + \text{C}_6\text{H}_6$ system (bond lengths in Å).

valence orbital populations of atom X in the adduct (Table 5). With one exclusion (the $\text{MeH}_2\text{C}-\text{C}_6\text{H}_6$ adduct), this decrease of population is followed by the rise of the transition-state levels for both channels. However, this is true only for adducts which form covalent σ X–Y bonds. The complexes of silylium cations with benzene are π -complexes and do not match this correlation.

Conclusions

1. All reactions $\text{R}'\text{R}''\text{HX}^+ + \text{YH} \rightarrow [\text{R}'\text{R}''\text{X}-\text{Y}]^+ + \text{H}_2$ (I) and $\text{R}'\text{R}''\text{HX}^+ + \text{YH} \rightarrow [\text{R}'\text{HX}-\text{Y}]^+ + \text{CH}_4$ (II) ($\text{R}'\text{R}'' = \text{CH}_3, \text{H}$; $\text{X} = \text{C}, \text{Si}$; $\text{Y} = \text{CH}_3\text{O}, (\text{CH}_3)_2\text{N}$, and C_6H_5) are exothermic and go through formation of intermediates (adducts). The association energies of these adducts decrease with methyl group substitution at X, but this decrease for $\text{X} = \text{Si}$ is substantially smaller than that for C. As a result, for systems with $(\text{CH}_3)_2\text{HX}^+$, the formation energy of the adduct with $\text{X} = \text{Si}$ becomes larger than those for $\text{X} = \text{C}$.

2. The mechanism of H_2 and CH_4 elimination from the adduct is similar for all systems studied. The first step for both channels is the migration of a H atom from the YH moiety to X. The transition-state structures along these paths may be described as a $[\text{R}'\text{R}''\text{X}-\text{Y}]^+$ ion with trivalent X and two hydrogens (or one hydrogen and a methyl group) coordinated to it. The relative barrier heights of the transition states for both channels depend primarily on the retention power of the X atom. The withdrawal of valence electrons from X by methyl substitution diminishes

Table 4. Relative Energies in kcal/mol (ΔE_{e} , $\Delta E_0 = \Delta E_{\text{e}} + \Delta \text{ZPVE}$) for Stationary Points of $\text{R}'\text{R}''\text{HX}^+ + \text{C}_6\text{H}_6$ Systems ($\text{R}', \text{R}'' = \text{CH}_3, \text{H}$)

		X = C			X = Si		
	no. ^a	ΔE_{e}	ΔE_0		no. ^a	ΔE_{e}	ΔE_0
H ₃ X ⁺							
reactants		0	0		0	0	
adduct	33	−86.9	−82.5	35	−52.3	−49.3	
TS	TS21	−44.7	−44.3	TS22	−6.7	−7.2	
complex	34	−65.0	−66.8	36	−28.0	−28.9	
products		−64.3	−67.0		−23.9	−27.1	
CH ₃ H ₂ X ⁺							
reactants		0	0		0	0	
adduct	37	−45.0	−41.2	40	−40.9	−38.0	
channel for H ₂ elimination (I)							
TS	TS23	−7.3	−6.6	TS25	1.5	0.9	
complex	38	−34.9	−37.4	41	−20.3	−21.6	
products		−34.0	−37.6		−17.7	−21.0	
channel for CH ₄ elimination (II)							
TS	TS24	−7.9	−6.7	TS26	5.7	5.0	
complex	39	−41.3	−40.0	42	−23.6	−22.2	
products		−39.8	−39.2		−17.9	−17.7	
(CH ₃) ₂ HX ⁺							
reactants		0	0		0	0	
adduct	43	−23.8	−19.5	46	−31.3	−28.5	
channel for H ₂ elimination (I)							
TS	TS27	12.1	13.4	TS29	8.6	8.1	
complex	44	−19.3	−22.2	47	−14.1	−15.8	
products		−18.8	−22.3		−12.1	−15.6	
channel for CH ₄ elimination (II)							
TS	TS28	10.7	12.3	TS30	12.9	12.2	
complex	45	−31.4	−30.0	48	−17.6	−16.6	
products		−30.0	−29.3		−14.1	−14.0	

^a Structure numbers as in Figures 11–15.

Table 5. Correlation of the ΔE_0^{TS} Values (kcal/mol) for Transition States for the Reactions I^a and II^b with the Natural Population of Valence Orbitals (ρ_v) of X Atoms of Corresponding Intermediates (Adducts)

R'	R''	Y	X = C			X = Si		
			ρ_v	ΔE_0^{TS}		ρ_v	ΔE_0^{TS}	
				I	II		I	II
H	H	C_6H_5	4.597	−44.3		2.995	−7.2	
H	H	$(\text{CH}_3)_2\text{N}$	4.404	−33.5		2.918	−18.8	
H	H	CH_3O	4.241	−13.1		2.817	−13.1	
CH_3	H	C_6H_5	4.379	−6.6	−6.7	2.717	0.9	5.0
CH_3	H	$(\text{CH}_3)_2\text{N}$	4.203	1.1	−3.4	2.653	−12.7	−11.2
CH_3	CH_3	C_6H_5	4.193	13.4	12.3	2.432	8.1	12.2
CH_3	H	CH_3O	4.050	16.4	10.3	2.564	−9.2	−9.9
CH_3	CH_3	$(\text{CH}_3)_2\text{N}$	4.021	19.2	13.6	2.380	−7.0	−5.2
CH_3	CH_3	CH_3O	3.871	30.9	26.3	2.306	−5.0	−5.2

^a Reaction I: $\text{R}'\text{R}''\text{HX}^+ + \text{YH} \rightarrow [\text{R}'\text{R}''\text{X}-\text{Y}]^+ + \text{H}_2$. ^b Reaction II: $\text{R}'(\text{CH}_3)\text{HX}^+ + \text{YH} \rightarrow [\text{R}'\text{HX}-\text{Y}]^+ + \text{CH}_4$. Italics are for the silylium ion–benzene systems, the barrier heights for which do not match the correlation.

this power. The propensity of silicon for coordination-sphere expansion makes the barrier heights for these transition states lower than those for $\text{X} = \text{C}$.

3. For systems with $\text{X} = \text{C}$, the relative transition-state energies with respect to the reactant energy levels (ΔE_0^{TS}) correlate well with natural populations of the valence orbitals of the X atom: the decrease of this population with H/Me substitution at X leads to the growth of ΔE_0^{TS} . For adducts with $\text{X} = \text{Si}$, a similar correlation is valid only for $\text{Y} = (\text{CH}_3)_2\text{N}$ and $\text{Y} = \text{CH}_3\text{O}$. Complexes of silylium cations with benzene have a different nature from the rest of the adducts studied, and their barrier heights do not match this correlation.

4. In adducts formed by the condensation of carbenium ions with methanol and dimethylamine, the unimolecular decomposition is formally allowed ($\Delta E_0^{\text{TS}} < 0$) only for the methyl cation, while for silylium cations studied, all adducts have $\Delta E_0^{\text{TS}} < 0$. For systems with benzene, only adducts with H_3X^+ have transition states for H_2 elimination below reactants for both C or Si.

5. Product (exit) complexes for H_2 elimination are very weakly bound, and the majority of them are unbound after ZPVE corrections. However, complexes with methane are substantially stronger, especially for $\text{X} = \text{Si}$, and their complexation energy may reach 8 kcal/mol ($[\text{H}_2\text{SiOCH}_3 \cdot \text{CH}_4]^+$). In the latter complex the $\text{Si} \cdots \text{H}$ interatomic separation is only 2.02 Å. As with ΔE_0^{TS} , the stability of product complexes decreases with the number of methyl groups at X and in the order $\text{CH}_3\text{OH} > \text{C}_6\text{H}_6 > (\text{CH}_3)_2\text{NH}$.

6. An important effect in silicon chemistry is the fact that the σ^* (Si–C) orbital is lower in energy than the corresponding

C–C σ^* orbital. There can thus be a strong hyperconjugative effect weakening the Si–C bond. This is a significant reason for the π -complex character in the case of $\text{R}_3\text{Si}-\text{C}_6\text{H}_6^+$. This effect also plays a role as soon as the proton leaves O or N, and lone-pair delocalization supports the breaking of the second X–H bond. For $\text{X} = \text{Si}$, this description is more effective, and therefore the transition-state energies are lower.

7. The final complexes may be viewed as donor (H–H or $\text{H}_3\text{C}-\text{H}$)–acceptor complexes, where the acceptor ability depends on the delocalization of adjacent lone-pair electrons into the empty orbital at X. For $\text{X} = \text{C}$, the delocalization is stronger: $(2\pi/2\pi)$ overlap for carbon is better than $(2\pi/3\pi)$ overlap for silicon. Hence, silicon is the better acceptor.

Acknowledgment. This research was supported by the National Science Foundation, Grant CHE-0136186.

JA040127E